

## Differential Degradation of Amyloid $\beta$ Genetic Variants Associated with Hereditary Dementia or Stroke by Insulin-degrading Enzyme\*

Received for publication, January 9, 2003, and in revised form, March 18, 2003  
Published, JBC Papers in Press, April 14, 2003, DOI 10.1074/jbc.M300276200

Laura Morelli‡, Ramiro Llovera‡, Silvia A. Gonzalez§, José L. Affranchino§, Frances Prelli¶, Blas Frangione¶, Jorge Ghiso¶, and Eduardo M. Castaño‡||

From the ‡Instituto de Química y Físicoquímica Biológicas (IQUIFIB), Consejo Nacional de Investigaciones Científicas y Técnicas (CONICET), Cátedra de Química Biológica Patológica, Departamento de Química Biológica, Facultad de Farmacia y Bioquímica, Universidad de Buenos Aires, Junin 956, C1113AAD, Buenos Aires, Argentina, §Centro de Virología Animal, CONICET, Serrano 665, Buenos Aires, Argentina, and ¶Department of Pathology, New York University School of Medicine, New York, New York 10016

**Inherited amino acid substitutions at position 21, 22, or 23 of amyloid  $\beta$  ( $A\beta$ ) lead to presenile dementia or stroke. Insulin-degrading enzyme (IDE) can hydrolyze  $A\beta$  wild type, yet whether IDE is capable of degrading  $A\beta$  bearing pathogenic substitutions is not known. We studied the degradation of all of the published  $A\beta$  genetic variants by recombinant rat IDE (rIDE). Monomeric  $A\beta$  wild type, Flemish (A21G), Italian (E22K), and Iowa (D23N) variants were readily degraded by rIDE with a similar efficiency. However, proteolysis of  $A\beta$  Dutch (E22Q) and Arctic (E22G) was significantly lower as compared with  $A\beta$  wild type and the rest of the mutant peptides. In the case of  $A\beta$  Dutch, inefficient proteolysis was related to a high content of  $\beta$  structure as assessed by circular dichroism. All of the  $A\beta$  variants were cleaved at Glu<sup>3</sup>-Phe<sup>4</sup> and Phe<sup>4</sup>-Arg<sup>5</sup> in addition to the previously described major sites within positions 13–15 and 18–21. SDS-stable  $A\beta$  dimers were highly resistant to proteolysis by rIDE regardless of the variant, suggesting that IDE recognizes a conformation that is available for interaction only in monomeric  $A\beta$ . These results raise the possibility that upregulation of IDE may promote the clearance of soluble  $A\beta$  in hereditary forms of  $A\beta$  diseases.**

The accumulation of amyloid  $\beta$  peptide ( $A\beta$ )<sup>1</sup> in the brain is a central process in a number of human neurodegenerative disorders that may be grouped as “amyloid  $\beta$  diseases” (1). In Alzheimer’s disease,  $A\beta$  is mainly found within senile plaques

\* This work was supported in part by Beca Carrillo Oñativia, Ministerio de Salud (to E. M. C. and L. M.), Agencia Nacional de Promoción Científica y Tecnológica Grant PICT98-05-04394 (to L. M. and E. M. C.), Fulbright Scholar Program fellowship (to L. M.), International Society for Neurochemistry-Committee for Aid and Education in Neurochemistry Award (to E. M. C.), and National Institutes of Health Grants AG10491, AG08721, and NS38777. The costs of publication of this article were defrayed in part by the payment of page charges. This article must therefore be hereby marked “advertisement” in accordance with 18 U.S.C. Section 1734 solely to indicate this fact.

|| To whom correspondence should be addressed: IQUIFIB, CONICET, Cátedra de Química Biológica Patológica, Departamento de Química Biológica, Facultad de Farmacia y Bioquímica, Universidad de Buenos Aires, Junin 956, C1113AAD, Buenos Aires, Argentina. Tel.: 54-11-4-964-8288; Fax: 54-11-4-962-5457; E-mail: edcast@ffyb.uba.ar.

<sup>1</sup> The abbreviations used are:  $A\beta$ , amyloid  $\beta$ ;  $A\beta$  PP, amyloid  $\beta$  precursor protein; IDE, insulin-degrading enzyme; rIDE, recombinant insulin-degrading enzyme; Tricine, *N*-[2-hydroxy-1,1-bis(hydroxymethyl)ethyl]glycine; WT, wild type; GST, glutathione *S*-transferase; CD, circular dichroism; MALDI-TOF MS, matrix-assisted laser desorption ionization time-of-flight mass spectrometry; HCHWA-D, hereditary cerebral hemorrhage with amyloidosis, Dutch type.

in the neurophil and vascular lesions, whereas in sporadic and hereditary amyloid angiopathies,  $A\beta$  deposits are mainly associated with cortical and leptomeningeal vessels leading to stroke or multi-infarct dementia. To a lesser extent, cerebral  $A\beta$  deposits are also present in normal aging (2). Autosomal dominant mutations in the amyloid  $\beta$  precursor protein ( $A\beta$  PP) gene result in amino acid substitutions at position 21, 22, or 23 of  $A\beta$  sequence. Although these  $A\beta$  variants present with a primarily vascular deposition, they translate into different clinical phenotypes. In this regard,  $A\beta$  Arctic (E22G) and  $A\beta$  Iowa (D23N) are characterized by presenile dementia and  $A\beta$  Flemish (A21G) is associated with early onset dementia and cerebral hemorrhage, whereas  $A\beta$  Dutch (E22Q) and  $A\beta$  Italian (E22K) variants have a predominant vascular phenotype characterized by massive strokes (3–7). The underlying mechanism of aggregation and deposition *in vivo* may be strongly influenced by the type of amino acid substitution as well as the location of mutations in the  $A\beta$  peptide. *In vitro* studies have shown that  $A\beta$  E22Q and  $A\beta$  D23N form typical amyloid fibrils at a higher rate than wild-type  $A\beta$  and that  $A\beta$  E22G assembles into unique protofibrils that may be toxic to neurons (3, 8–10). In the case of  $A\beta$  A21G, overproduction of the peptide may contribute as a pathogenic mechanism (11, 12). Regarding  $A\beta$  E22K, deposition seems not to be related with fibril formation rate, and yet this variant may be toxic to human cerebrovascular smooth muscle cells in culture (6, 13). In addition to the intrinsic aggregation properties of  $A\beta$  and its genetic variants or the rate of their production, recent studies (14, 15) in animal models have suggested that a defective clearance may influence the progressive accumulation of  $A\beta$  in the neurophil and cerebral vessels. Among the mechanisms that remove  $A\beta$  peptides from the brain, degradation by several proteases including neprilysin, endothelin-converting enzyme, and insulin degrading enzyme (IDE) is now being considered as an important component of the  $A\beta$  clearance process (16, 17, reviewed in Refs. 18 and 19). IDE is a highly conserved thiol metalloprotease with ubiquitous expression including the brain (20–22). Regarding its physiological role, IDE has been implicated in cellular growth and differentiation, modulation of proteasomal activity, and steroid signaling (23, reviewed in Ref. 24). In addition to insulin for which the protease has a  $K_m$  in the low nanomolar range, IDE is known to degrade several peptides capable of forming amyloid fibrils *in vitro* and *in vivo* including glucagon, amylin, atrial natriuretic peptide, calcitonin, and  $A\beta$  (25, 26, reviewed in Ref. 27). Studies using rat and human brain tissue homogenates, IDE-transfected cell lines, and primary neuronal cultures have supported a role of IDE in  $A\beta$  degradation *in vivo* (28–31). Moreover, IDE has been shown to

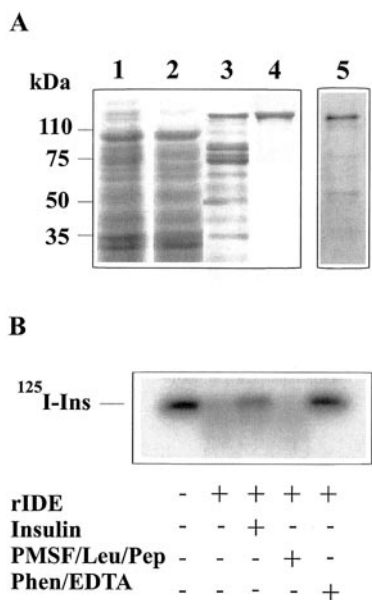


**FIG. 1. Characterization of recombinant rat IDE.** *Panel A*, SDS-PAGE and Coomassie Blue staining (*lanes 1–4*) of proteins obtained during the purification procedure of rIDE. *Lane 1*, total bacterial lysate; *lane 2*, proteins unbound to Ni column; *lane 3*, eluate with 100 mM imidazole; *lane 4*, eluate with 400 mM imidazole; *lane 5*, Western blot of purified rIDE using BC2 polyclonal antiserum. *Left*, molecular mass markers in kilodaltons. *Panel B*, SDS-PAGE and PhosphorImager analysis of [<sup>125</sup>I]insulin degradation by rIDE in the presence or absence of different inhibitors as indicated. Unlabeled insulin was used at 1  $\mu$ M. *Leu*, leupeptin; *Pep*, pepstatin; *Phen*, 1,10-phenanthroline.

protect cultured neurons from A $\beta$  toxicity, indicating that the A $\beta$  fragments generated by IDE are not themselves toxic to cells (32). Regarding the state of A $\beta$  oligomerization and IDE specificity, it has been proposed that IDE is able to degrade efficiently monomeric A $\beta$  as opposed to oligomeric A $\beta$  species that are thought to be more toxic to neurons or vascular cells than typical amyloid fibrils (33). However, whether IDE is capable of degrading A $\beta$  bearing pathogenic amino acid substitutions and how these changes may affect specificity is not known. The aim of our work was to study the degradation of A $\beta$  genetic variants associated with human disease by recombinant IDE *in vitro* and to characterize the proteolytic products from each of these A $\beta$  mutant peptides.

#### EXPERIMENTAL PROCEDURES

**Expression and Purification of Recombinant Rat IDE**—The plasmid pECE-IDE (kindly provided by Richard Roth, Stanford University), containing the coding region of rat IDE cDNA was used as a template for the PCR amplification of a truncated version of IDE using sense 5'-AGCACAGGATCCATGAATAATCCGGCCAT-3' (nucleotides 139–155) and antisense 5'-TTCTCGAGGAGTTTTCGCCCATGA-3' (nucleotides 3072–3056) primers of the rat IDE cDNA sequence. Sites for the restriction enzymes *Bam*HI and *Xho*I, respectively, were introduced to facilitate cloning. The PCR DNA fragment was digested with *Bam*HI and *Xho*I and cloned into pET-30a(+) (Novagen) previously digested with the same restriction enzymes to generate the pET-IDE construct. Recombinant IDE 42-1019 (rIDE) was expressed in *Escherichia coli* BL21 and purified to homogeneity using a Hi Trap Ni-chelating column (Amersham Biosciences) following the method described by Chesneau and Rosner (34). Purity, as assessed by SDS-PAGE, was >95%. rIDE proteolytic activity was determined using [<sup>125</sup>I]insulin as described below.

**Production of Anti-IDE Polyclonal Antibodies**—A region between amino acids 97 and 273 of the rat IDE sequence was amplified by PCR using as template pECE-IDE with the following primers: forward 5'-CTGAGCGGATCCCTGTCCAGACCTCCA-3' and reverse 5'-CAATGTGAATTCCTTCCACCAGATT-3'. After digestion with *Bam*HI and *Eco*RI, the 530-bp insert was subcloned into pGex2T vector (Amersham Biosciences). GST-IDE97–273 fusion protein was expressed and purified according to the manufacturer's suggestions. After immunization of

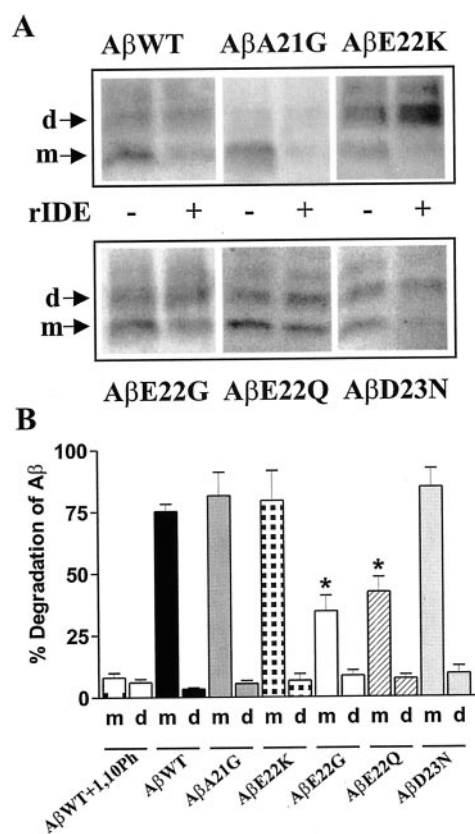


**FIG. 2. Degradation of A $\beta$  variants by rIDE.** *Panel A*, Western blot analysis with monoclonal 6E10 of degradation of A $\beta$  WT and A $\beta$  genetic variants by rIDE. *m*, A $\beta$  monomers; *d*, A $\beta$  dimers. *Panel B*, densitometric quantitation of the immunoreactivity of A $\beta$  as in panel A. *m*, monomers; *d*, dimers. *Bars* represent the mean  $\pm$  S.E. of three independent experiments. \*,  $p < 0.01$  (Student's *t* test) as compared with A $\beta$  WT.

New Zealand rabbits with GST-IDE97–273, the antiserum (BC2) was sequentially purified using a BL21/GST lysate coupled to CNBr-activated Sepharose (Amersham Biosciences) and a GST-agarose (Sigma) affinity columns, respectively. Specificity of anti-IDE antiserum BC2 was tested by Western blot against GST, GST-IDE97–273, purified rIDE (see above), and soluble fractions from human and rat brain and liver in which a single 115-kDa band was detected (data not shown).

**Synthetic Peptides**—Synthetic A $\beta$ (1–40)-peptides such as A $\beta$  WT, A $\beta$  A21G, A $\beta$  E22Q, A $\beta$  E22K, A $\beta$  E22G, A $\beta$  D23N, and A $\beta$ (1–40)/A $\beta$ (1–42) containing the rodent sequence (35) were synthesized by the W. M. Keck Foundation (Yale University, CT). All of the peptides were purified by reverse-phase high pressure liquid chromatography, and their purity was evaluated by amino acid sequence analysis and laser desorption mass spectrometry. Lyophilized aliquots of the peptides were dissolved at a concentration of 70  $\mu$ M in distilled water as determined with a bicinchoninic acid assay (Pierce) after centrifugation at 10,000 rpm for 15 min to eliminate large aggregates. The supernatant was aliquoted and stored at  $-80^{\circ}$ C.

**SDS-PAGE and Western Blot**—Proteins obtained from *E. coli* BL21 lysates and after the different steps of purification were analyzed by 7.5% SDS-PAGE in Tris-Tricine gels. A $\beta$  peptides were run on 12.5% Tris-Tricine SDS-PAGE. For Western blot analysis, proteins were transferred onto nitrocellulose membranes (Hybond ECL, Amersham Biosciences) and incubated with anti-A $\beta$  monoclonal antibody 6E10 (Signet Laboratories) at 1:1000, anti-IDE monoclonal 9B12 (kindly provided by Richard Roth) at 1:1000, and polyclonal antibody BC2 at 1:1000. Immunoreactivity was detected with anti-mouse or anti-rabbit horseradish peroxidase-labeled IgG and ECL Plus (Amersham Biosciences). Immunoblots were scanned with STORM 840 and analyzed with ImageQuant 5.1 software (Amersham Biosciences).

**In-gel Tryptic Digestion of rIDE and Amino Acid Sequencing**—After SDS-PAGE and Coomassie Blue staining, the band of 125 kDa was cut and the gel slice was incubated in 100 mM ammonium bicarbonate, pH 8.3 containing 45 mM dithiothreitol for 30 min at 60  $^{\circ}$ C. The tube was cooled at room temperature, and 100 mM iodoacetamide was added

TABLE I  
Mass spectrometry analysis of the cleavage products of A $\beta$  variants by insulin-degrading enzyme

NF, not found; Obs., observed; Calc., calculated.

A $\beta$ fragment	Molecular mass of A $\beta$ variants													
	A $\beta$ WT		A $\beta$ A21G		A $\beta$ E22K		A $\beta$ E22Q		A $\beta$ E22G		A $\beta$ D23N		A $\beta$ rodent	
	Obs.	Calc.	Obs.	Calc.	Obs.	Calc.	Obs.	Calc.	Obs.	Calc.	Obs.	Calc.	Obs.	Calc.
	<i>Da</i>													
1–13	1561.8	1561.6	NF		1562.6	1561.6	1561.9	1561.3	1562.2	1561.6	1562.1	1561.6	1466.3	1465.5
1–14	1699	1698.3	1699.5	1693.7	1699.9	1698.7	1699.5	1698.7	1699.4	1698.7	1699.3	1698.7	1603.7	1602.6
1–18	2167.9	2167.3	NF		2165.6	2167.3	NF		2168.9	2167.3	2168.1	2167.3	2072.9	2071.2
1–19	2315.1	2314.5	2315.6	2314.5	NF		NF		2315.7	2314.5	2315.3	2314.5	2220.2	2218.4
1–20	2462.6	2461.7	NF		2462.9	2461.7	NF		NF		NF		NF	
1–26	NF		NF		NF		NF		NF		3019.2	3019.2	NF	
1–28	NF		NF		NF		NF		NF		3261.3	3261.5	3168.2	3166.5
4–13	1246.4	1246.3	1246.8	1246.3	1247	1246.3	1246.7	1246.3	1246.7	1246.3	1246.7	1246.3	1151.2	1150.2
4–14	1383.7	1383.5	1384	1383.5	1384.2	1385.5	1384	1383.4	1384	1383.5	1383.9	1385.5	NF	
4–19	2000	1999.2	NF		NF		NF		NF		NF		NF	
5–14	1236.3	1236.3	1236.8	1236.3	1237	1236.3	1236.6	1236.3	1236.6	1236.3	1236.6	1236.3	NF	
14–20	NF		NF		NF		918.9	918.1	NF		NF		NF	
14–28	1719.4	1718.9	1705.8	1704.9	NF		NF		1647.4	1646.9	NF		NF	
15–26	NF		NF		NF		NF		NF		1338.6	1338.5	NF	
15–28	1582	1581.8	1568.3	1567.8	NF		NF		1510.5	1509.7	NF		NF	
15–40	NF		NF		2650.5	2648.2	NF		2578.5	2579.1	NF		NF	
19–28	NF		1100.2	1099.2	NF		NF		NF		NF		NF	NF
19–40	2180.4	2180.6	NF		NF		NF		NF		NF		NF	NF
20–40	NF		2020.3	2019.4	2033.5	2032.4	2033.8	2032.4	1962.1	1961.3	2033.1	2032.3	2034.6	2033.5
21–40	NF		NF		1886.6	1885.3	1886.5	1885.2	1814.6	1814.1	1885.7	1885.2	1887.5	1886.2
27–40	NF		NF		NF		NF		NF		1327.7	1327.7	NF	NF
29–40	NF		1084.9	1085.4	NF		NF		1085.5	1086	NF		NF	NF

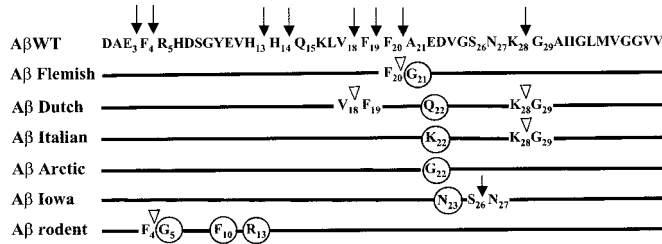


FIG. 3. Schematic representation of cleavage sites within A $\beta$  WT, A $\beta$  rodent, and A $\beta$  human genetic variants by rIDE. Arrows show the peptide bonds hydrolyzed by rIDE. Open arrowheads ( $\nabla$ ) indicate loss of cleavage under the experimental conditions tested. The lines represent identity of amino acid sequence and cleavage sites. Amino acid substitutions in each A $\beta$  variant are shown in circles.

followed by incubation for 30 min in the dark at room temperature. The gel was then washed in 50% acetonitrile, 100 mM ammonium bicarbonate with shaking for 1 h, cut in pieces, and transferred to a small tube. Acetonitrile was added to shrink the gel pieces, and the sample was dried in a rotatory evaporator. The gel pieces were re-swollen with 10  $\mu$ l of 100 mM ammonium bicarbonate, pH 8.3, containing trypsin at a 10:1 ratio (w/w, substrate:enzyme). The sample was incubated overnight at 37  $^{\circ}$ C, and digestion products were extracted twice from the gel with 60% acetonitrile, 0.1% trifluoroacetic acid for 20 min. Combined extractions were loaded into a C<sub>18</sub> high pressure liquid chromatography column (220  $\times$  1 mm), and peptides eluted with a linear gradient from 0 to 100% acetonitrile, 0.1% trifluoroacetic acid. Selected peaks were applied to a 477A protein-peptide sequencer (Applied Biosystems) and subjected to Edman degradation sequence analysis at the Laboratorio Nacional de Investigacion y Servicios en Péptidos y Proteinas facility (CONICET).

**Degradation Assays**—1  $\mu$ g of each A $\beta$  synthetic peptide was incubated alone or with 500 ng of purified rIDE in 10  $\mu$ l of 100 mM sodium phosphate buffer, pH 7, in the presence or absence of 1 mM 1,10-phenanthroline. After 30, 60, 90, and 120 min of incubation at 37  $^{\circ}$ C, samples were analyzed by SDS-PAGE and Western blot with 6E10 as described above. After each time point, degradation by rIDE was expressed as the percentage of remaining A $\beta$  monomer or dimer as compared with A $\beta$  incubated without the enzyme. [<sup>125</sup>I]Insulin (specific activity 300  $\mu$ Ci/ $\mu$ g, kindly provided by Edgardo Poskus, University of Buenos Aires.) was incubated with rIDE alone or in the presence of the following sets of inhibitors: 1) 1  $\mu$ M unlabeled insulin; 2) a mixture of 2 mM phenylmethylsulfonyl fluoride, 10  $\mu$ g/ml leupeptin, and 10  $\mu$ g/ml pepstatin A; 3) a mixture of 1 mM 1,10-phenanthroline and 5 mM EDTA,

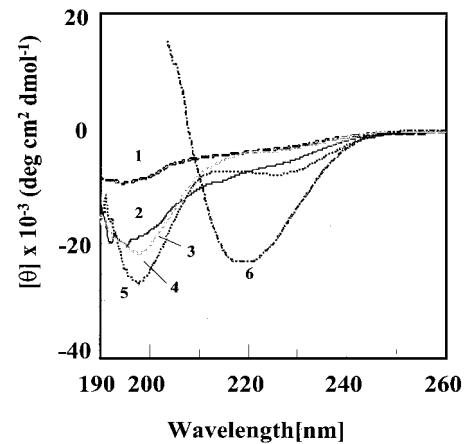


FIG. 4. Circular dichroism spectra of A $\beta$  variants. Aliquots (400  $\mu$ g) of each peptide were dissolved in 1.5 ml of 10 mM Tris-HCl buffer, pH 7.5. After centrifugation at 14,000 rpm for 5 min to remove aggregates, CD spectra were recorded in a JASCO spectropolarimeter J-720 in a 0.1-cm path length cell. Results are expressed as mean residue ellipticity in units of deg cm<sup>2</sup> dmol<sup>-1</sup> after subtraction of buffer spectra and smoothing with algorithm provided by JASCO. Spectra: 1, A $\beta$  E22G; 2, A $\beta$  WT; 3, A $\beta$  D23N; 4, A $\beta$  A21G; 5, A $\beta$  E22K and 6, A $\beta$  E22Q.

respectively, in the same buffer as above. After incubation for various time points, the sample was run on SDS-PAGE, and the remaining intact [<sup>125</sup>I]insulin was analyzed and quantitated with a STORM 840 PhosphorImager (Amersham Biosciences).

**Circular Dichroism (CD) Spectra**—Aliquots of A $\beta$  synthetic peptides freshly dissolved at 60  $\mu$ M in 10 mM Tris-HCl, pH 7.5, were loaded into a 0.1-nm path length quartz cell, and the circular dichroism spectra were recorded in the far-ultraviolet light using a JASCO J-720 spectropolarimeter (JASCO Corporation). Forty scans for each experimental condition were obtained at 0.2-nm intervals over the wavelength range of 190–260 nm. Final spectra were obtained after the subtraction of background readings of blanks.

**Mass Spectrometry Analysis**—Molecular masses of intact A $\beta$  peptides and the products of rIDE degradation were determined at the New York University Protein Analysis Facility. A $\beta$ -containing samples (10  $\mu$ l of final volume) were passed through reversed-phase ZipTip (Millipore) following manufacturer's instructions and analyzed on a Micro-mass ToFSpec-2E (MALDI-TOF) mass spectrometer in linear mode using standard instrument settings. Internal and/or external calibration

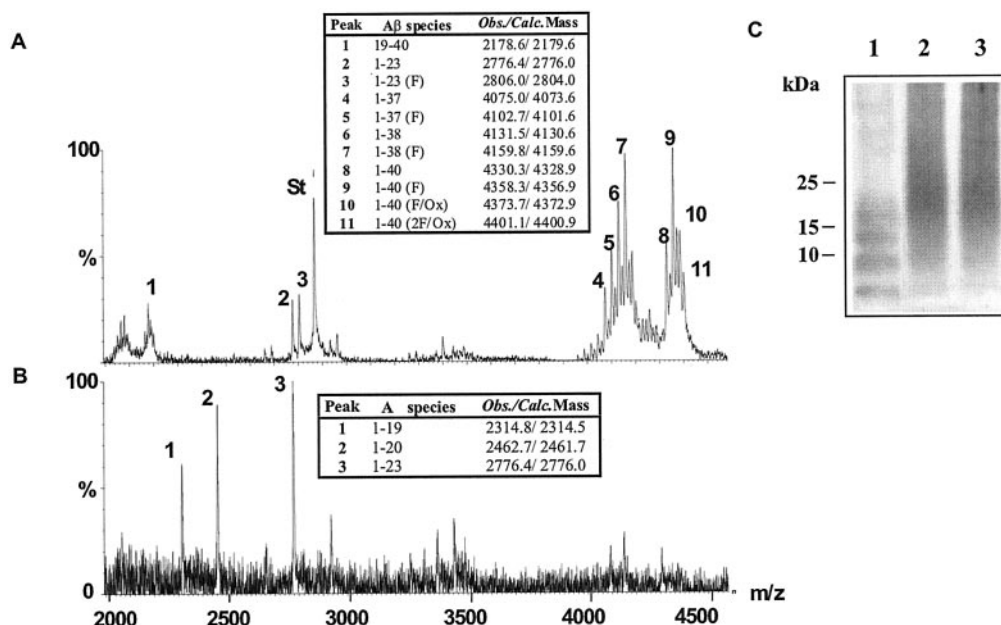


FIG. 5. **Degradation of A $\beta$  E22Q from HCHWA-D leptomeningeal vessels by rIDE.** MALDI-TOF MS analysis of native A $\beta$  E22Q extracted in formic acid after incubation for 1 h at 37 °C in the absence (panel A) or in the presence (panel B) of rIDE. *St*, standard (insulin mass/2H). *Insets*, calculated and observed masses of A $\beta$  E22Q species and predicted peptides. The presence of one or two formic acid molecules is indicated by F or 2F, respectively. *Panel C*, Western blot analysis with monoclonal 6E10 after incubation of A $\beta$  E22Q from HCHWA-D leptomeningeal vessels with rIDE. Synthetic A $\beta$  E22Q (lane 1) and HCHWA-D amyloid incubated for 1 h at 37 °C alone (lane 2) and with rIDE (lane 3) are shown. *Left*, molecular masses in kilodaltons.

was carried out using angiotensin I (average mass = 1296.5 Da) and insulin (average mass = 5733.5 Da).

**Isolation of A $\beta$  from Leptomeningeal Vessels**—Leptomeningeal vascular amyloid from a patient with hereditary cerebral hemorrhage with amyloidosis Dutch type (HCHWA-D) was isolated as described previously (36). Leptomeninges were dissected from brain coronal sections, cut with scissors into 1–3-mm pieces, and placed in 0.1 M Tris-HCl, pH 8, on ice. Tissue was then washed by resuspension in 0.1 M Tris-HCl, pH 8, containing protease inhibitors (buffer A) and centrifuged at 800  $\times$  *g* for 5 min at 4 °C. The procedure was repeated 5 times. The material was collected by filtration through a 50- $\mu$ m nylon mesh (Spectrum), washed with buffer A without inhibitors, and resuspended in 20 volumes of 2 mM CaCl<sub>2</sub> in 0.1 M Tris-HCl, pH 7.5, containing 0.3 mg/ml collagenase CLS-3 (Worthington) and 10  $\mu$ g/ml DNase (Worthington). The mixture was incubated for 18 h at 37 °C. After digestion, the suspension was filtered through a 350- $\mu$ m nylon mesh and the filtrate was centrifuged at 10,000  $\times$  *g* for 12 min. The pellet was resuspended in 2% SDS in 0.1 M Tris-HCl, pH 8, and incubated for 2 h at room temperature. The SDS-insoluble material was recovered by centrifugation as above and washed three times with distilled water. The pellet was dissolved in 10 volumes of 99% formic acid (Sigma) and incubated for 1 h at room temperature. After centrifugation at 10,000  $\times$  *g* for 10 min, the supernatant was then loaded on a Superose 12 column (10  $\times$  300 mm) (Amersham Biosciences). Amyloid peptides were separated in 75% formic acid at 0.2 ml/min using a Bio-Cad Sprint chromatography system. Eluent was monitored at 280 nm, collected in 1-ml fractions, and analyzed as above.

## RESULTS

**Expression and Characterization of Recombinant Rat IDE**—Our IDE bacterial expression vector pET-IDE encodes rat IDE (positions 42–1019) with a His<sub>6</sub> tag at its N terminus to facilitate the purification of the protease with a Ni-affinity column. After elution with a step gradient of increasing imidazole concentrations, we obtained a highly purified recombinant protein with an apparent molecular mass of 125 kDa as assessed by SDS-PAGE. Western blot using our polyclonal antibody BC2 specifically recognized this 125-kDa fusion protein (Fig. 1A). Unexpectedly, the protein did not display immunoreactivity on Western blot with monoclonal 9B12, a well characterized anti-rat IDE antibody (data not shown) (37). To determine its identity, we performed “in-gel” digestion with trypsin followed by

separation on microbore high pressure liquid chromatography and N-terminal amino acid sequence of a tryptic fragment. The sequence NVPLPEF matched positions 282–288 of rat IDE (20), confirming the identity of our recombinant protease and suggesting that 9B12 may indeed recognize a posttranslationally modified epitope in rat IDE that is not present in IDE expressed in bacteria. To characterize the activity of recombinant rIDE, we analyzed the degradation of [<sup>125</sup>I]insulin. After 1 h of incubation, rIDE was able to digest [<sup>125</sup>I]insulin and this activity was totally inhibited by EDTA-1,10-phenanthroline and blocked to 80% in the presence of 1  $\mu$ M unlabeled insulin (Fig. 1B). These results are fully consistent with the reported characterization of human recombinant IDE expressed in *E. coli* (34) and rat recombinant IDE produced in a baculovirus-insect cell system (32).

**Degradation of A $\beta$  WT and A $\beta$  Genetic Variants by rIDE**—We followed the degradation of A $\beta$  WT and A $\beta$  genetic variants by rIDE using SDS-PAGE and Western blot with monoclonal 6E10 that recognizes an epitope within positions 1–16 of A $\beta$  (38). The relative amount of A $\beta$  monomers and dimers that remained intact after incubation with rIDE was estimated by densitometry. This method allowed an accurate discrimination between monomeric and oligomeric A $\beta$  as opposed to high pressure liquid chromatography or trichloroacetic acid precipitation (28, 29). The absence of A $\beta$  degradation products on Western blots may reflect the loss of the 6E10 epitope attributed to rIDE activity. Alternatively, the A $\beta$  N-terminal fragments generated by the protease may be too small to be detected on SDS-PAGE. Under the conditions of our assay, the quantitation of degradation showed linearity up to 90 min of incubation (data not shown); therefore, a 60-min incubation was the time selected for the comparative analysis. As indicated in Fig. 2, A and B, monomeric A $\beta$  WT, A $\beta$  A21G, A $\beta$  E22K, and A $\beta$  D23N were degraded at 75.2  $\pm$  3, 81.5  $\pm$  9.2, 79.5  $\pm$  12, and 84.7  $\pm$  7.6%, respectively. rIDE was substantially less efficient in degrading A $\beta$  E22Q and A $\beta$  E22G monomers (42.3  $\pm$  6 and 34.6  $\pm$  6%, respectively, *p* < 0.01 as compared with A $\beta$  WT). In the presence of 1,10-phenanthroline, degradation of A $\beta$  WT was inhibited almost completely (Fig. 2B). In contrast to A $\beta$  monomers, degradation of

dimers was consistently <10% for all of the variants studied (Fig. 2B), in agreement with the results reported recently on endogenous A $\beta$  WT generated by A $\beta$  PP-transfected cell lines (33).

**Characterization of A $\beta$  Proteolytic Products**—A $\beta$  WT proteolytic products generated by rIDE were consistent with previous reports with the major sites of cleavage at His<sup>13</sup>-His<sup>14</sup>, His<sup>14</sup>-Gln<sup>15</sup>, Val<sup>18</sup>-Phe<sup>19</sup>, Phe<sup>19</sup>-Phe<sup>20</sup>, Phe<sup>20</sup>-Ala<sup>21</sup>, and Lys<sup>28</sup>-Gly<sup>29</sup> (28, 32, 39). All of the A $\beta$  fragments observed by MALDI-TOF MS are summarized in Table I, and Fig. 3 shows a schematic representation of the cleavage sites. Several fragments starting at Phe<sup>4</sup> and Arg<sup>5</sup> were found in A $\beta$  WT and in all of the A $\beta$  variants. These peptides were not the products of truncated synthesis as shown by MS analysis of undigested A $\beta$  peptides and were not found when A $\beta$ s were incubated with rIDE in the presence of 1,10-phenanthroline (data not shown). Moreover, Phe and Arg as P1' residues are compatible with the known specificity of IDE (28, 41). Therefore, it seemed probable that rIDE was capable of hydrolyzing A $\beta$  Glu<sup>3</sup>-Phe<sup>4</sup> and Phe<sup>4</sup>-Arg<sup>5</sup> peptide bonds. In A $\beta$  A21G, there was a consistent absence of fragments ending at Phe<sup>20</sup> or starting at Gly<sup>21</sup>, suggesting the specific loss of a cleavage site. Notably, when we analyzed the digestion of rodent A $\beta$  that present Gly instead of Arg at position 5, no fragments indicative of hydrolysis at the Phe<sup>4</sup>-Gly<sup>5</sup> site were found, neither in rodent A $\beta$ -(1-40) (Table I and Fig. 3) nor in rodent A $\beta$ -(1-42) (data not shown), whereas all of the other cleavage sites present in human A $\beta$  WT were conserved. The Dutch variant A $\beta$  E22Q showed the apparent loss of sites at Val<sup>18</sup>-Phe<sup>19</sup> and Lys<sup>28</sup>-Gly<sup>29</sup>, whereas in the Italian variant A $\beta$  E22K, the latter cleavage site was also absent. This peptide bond has been reported to be resistant to IDE in A $\beta$  WT-(1-42) (32), and therefore, its hydrolysis by IDE may depend upon oligomerization rather than primary structure. Alternatively, the presence of Gly at P1' may impose a subsite restriction as suggested by the loss of cleavage sites in the A $\beta$  Flemish and rodent variants. The Iowa type A $\beta$  D23N differed notably from all of the other A $\beta$  peptides studied. Fragments consistent with positions 1-26, 15-26, and 27-40 were found, indicating the cleavage at the Ser<sup>26</sup>-Asn<sup>27</sup> bond (Table I and Fig. 3) and pointing to the possible importance of the Asp<sup>23</sup> in the folding of the A $\beta$  peptide.

**Effect of A $\beta$  Secondary Structure upon Degradation by rIDE**—To study the possible influence of secondary structure of A $\beta$  variants on the susceptibility to degradation by rIDE, we performed CD analysis of all of the peptides freshly dissolved in aqueous buffer at neutral pH without previous incubation and after the removal of large aggregates by centrifugation. As expected, A $\beta$  E22Q displayed a negative peak at 220 nm and a positive peak at 195 nm consistent with a  $\beta$  structure in solution (6). In contrast, A $\beta$  WT, A $\beta$  A21G, A $\beta$  E22G, A $\beta$  E22K, and A $\beta$  D23N showed a strong negative peak at 198 nm corresponding to unordered structures (Fig. 4).

**Degradation of A $\beta$  E22Q Purified from Leptomeningeal Vessels by rIDE**—To determine whether rIDE was capable of degrading the Dutch A $\beta$  variant present in affected human tissue, we used purified A $\beta$  from leptomeningeal vessels from a case of HCHWA-D that was extensively characterized previously (36). After the removal of formic acid by reverse-phase C<sub>18</sub> Zip Tip and equilibration of the sample at neutral pH, A $\beta$  Dutch was incubated with rIDE and degradation characterized as above. Western blot showed that A $\beta$  Dutch was extensively aggregated into SDS-resistant oligomers of ~22-25 kDa that were unmodified in the presence of rIDE (Fig. 5C). However, MALDI-TOF MS analysis revealed the disappearance of monomeric A $\beta$  Dutch and the generation of two fragments, positions 1-19 and 1-20 (Fig. 5, A and B), that were not seen in the presence of 1,10-phenanthroline (data not shown).

## DISCUSSION

Our results demonstrated that rIDE was capable of degrading all of the synthetic A $\beta$  variants associated with human disease and A $\beta$  Dutch purified from leptomeningeal vessels. However, the efficiency of degradation of synthetic A $\beta$  monomeric species by rIDE was significantly lower for A $\beta$  E22Q and A $\beta$  E22G as compared with A $\beta$  WT and the rest of the variant A $\beta$  peptides studied. The concentrations of A $\beta$  peptides used in our assays were above the critical concentration of A $\beta$ -(1-40) for the formation of high molecular weight oligomers (41), and therefore, it is likely that aggregation of A $\beta$  strongly influenced the rate of degradation by rIDE. In the case of the A $\beta$  Dutch variant, a possible slower rate of degradation could be explained by the high content of  $\beta$  structure as shown by CD analysis. This result was fully consistent with several *in vitro* studies that have demonstrated the fast rate of assembly into stable fibrils of this A $\beta$  mutant (8, 9, 36). The early deposition of A $\beta$  E22Q and onset of symptoms in HCHWA-D patients strongly suggest that such mechanism may be relevant *in vivo*. Moreover, the amyloidogenic conformation of A $\beta$  E22Q may be dominant because A $\beta$  WT has been also found in the HCHWA-D vascular deposits (42). The A $\beta$  Arctic variant peptide in turn has been shown to self-assemble rapidly into protofibrils that may be toxic to neural cells (3). Although the major quantitative differences in degradation were seen upon A $\beta$  E22Q and A $\beta$  E22G, it is unlikely that they reflect a protease-resistant conformation of these monomeric A $\beta$  species. The models based on NMR have shown a similar coiled flexible structure in aqueous solution for A $\beta$  E22Q and A $\beta$  WT (43, 44). Moreover, we have previously demonstrated that at physiological concentrations in the low nanomolar range, A $\beta$  WT and A $\beta$  E22Q were degraded at a similar rate by endogenous brain IDE (29). Thus, it seems more likely that monomeric A $\beta$  Dutch and Arctic variants were "hidden" from rIDE into higher oligomers or aggregates during incubation in physiological buffer that were then partially dissociated upon SDS treatment for Western blot analysis. It was notorious that all of the SDS-resistant A $\beta$  dimers including those from A $\beta$  WT were poorly degraded by rIDE, consistent with the resistance to proteolysis of native A $\beta$  WT-soluble oligomers in cultured cells overexpressing A $\beta$  PP (33). However, it cannot be concluded from these experiments whether A $\beta$  dimers or higher oligomers are the resistant species to degradation by rIDE. The separation of stable A $\beta$  oligomers by gel filtration under native conditions is needed to clarify this issue. In any case, our results and previous reports (28, 48) support that IDE recognizes a motif on monomeric A $\beta$  within positions 18-22, a known hydrophobic stretch that is critical for amyloid formation (45-47). It may be possible that when these residues participate in peptide self-assembly, they are no longer accessible to IDE catalytic site. Our findings on A $\beta$  D23N showed an apparent discrepancy with those presented recently by Van Nostrand *et al.* (10). In these reported experiments, A $\beta$  Iowa and A $\beta$  Dutch variants behaved similarly in terms of secondary structure and fibrillization rate after 48 h of incubation. Nevertheless, it is possible that at much shorter times of incubation, such as in our degradation and CD experiments, the rate of assembly into a  $\beta$  structure may be substantially faster for A $\beta$  E22Q as compared with A $\beta$  D23N, resulting in a higher resistance to proteolysis by rIDE. The A $\beta$  Iowa peptide was different among all of the A $\beta$  variants, because it presented a unique site of cleavage by rIDE at Ser<sup>26</sup>-Asn<sup>27</sup>. The possibility of multiple subsite interactions allowing different alignments of substrate relative to the site of catalysis in IDE has been recently demonstrated with the use of fluorogenic substrates (40). It remains to be addressed whether Asn instead of Asp at position 23 of A $\beta$ , being at P<sub>4</sub>

from Ser<sup>26</sup>-Asn<sup>27</sup>, may determine a new site of cleavage that seems atypical in light of the preference of IDE for hydrophobic and basic residues at P<sub>1</sub>' (27, 40). In addition to overproduction and an enhanced aggregability imposed by amino acid substitutions, A $\beta$  may accumulate in the brain due to defective clearance. In transgenic mice expressing human A $\beta$  PP with pathogenic mutations that promote the activity of  $\beta$ -secretase such as the double K670N/M671L substitution, the time course of amyloid deposition shows an exponential increase after 9–10 months of age (15, 49). Yet, the rate of A $\beta$  production and  $\beta$ -secretase activity seems to remain constant throughout the life span of these mice (14). A defect in reverse transport to the systemic circulation as shown for the A $\beta$  Dutch variant (50, 51) together with inefficient local proteolysis may determine a rise in the levels of A $\beta$  in the brain and therefore accelerate its rate of aggregation and deposition (16, 29, 52). In the case of human diseases associated with mutations clustered within the middle portion of A $\beta$ , such accumulation shows a remarkable predisposition for vessels in which A $\beta$  oligomers may be toxic to endothelial and smooth muscle cells. Our results *in vitro* raise the possibility that upregulation of IDE may promote the clearance of these A $\beta$  genetic variants *in vivo*. In this regard, it is noteworthy that A $\beta$  pathogenic mutants seem to be highly resistant to proteolysis by neprilysin *in vitro*, and therefore, increasing the activity of neprilysin may be inefficient to prevent A $\beta$  deposition in certain hereditary forms of amyloid  $\beta$  diseases (53). Yet, the apparent resistance of A $\beta$  oligomers to proteolysis by rIDE suggests that any strategy to lower A $\beta$  based on the enhancement of this endogenous protease should aim at the degradation of A $\beta$  at its monomeric state.

**Acknowledgment**—We thank Richard Roth (Stanford University) for the generous gift of pECE-IDE and 9B12 antibody.

## REFERENCES

- Castaño, E. M., and Frangione, B. (1988) *Lab. Invest.* **58**, 122–132
- Coria, F., Castaño, E. M., and Frangione, B. (1987) *Am. J. Pathol.* **129**, 422–428
- Nilsberth, C., Westlind-Danielsson, A., Eckman, C. B., Condrón, M. M., Axelman, K., Forsell, C., Stenh, C., Luthman, J., Teplow, D. B., Younkin, S. G., Naslund, J., and Lannfelt, L. (2001) *Nature Neurosci.* **4**, 887–893
- Kamino, K., Orr, H. T., Payami, H., Wijsman, E. M., Alonso, M. E., Pulst, S. M., Anderson, L., O'dahl, S., Nemens, E., White, J. A., Sadovnick, A. D., Ball, M. J., Kaye, J., Warren, A., McInnis, M., Antonarkis, S. E., Korenberg, J. R., Sharama, V., Kukull, W., Larson, E., Heston, L. L., Martin, G. M., Bird, T. D., and Schellenberg, G. D. (1992) *Am. J. Hum. Genet.* **51**, 998–1014
- Grabowski, T. J., Cho, H. S., Vonsattel, J. P., Rebeck, G. W., and Greenberg, S. M. (2001) *Ann. Neurol.* **49**, 697–705
- Miravalle, L., Tokuda, T., Chiarle, R., Giaccone, G., Bugiani, O., Tagliavini, F., Frangione, B., and Ghiso J. (2000) *J. Biol. Chem.* **275**, 27110–27116
- Levy, E., Carman, M. D., Fernandez-Madrid, I. J., Power, M. D., Lieberburg, I., van Duinen, S. G., Bots, G. T., Luyendijk, W., and Frangione, B. (1990) *Science* **248**, 1124–1126
- Wisniewski, T., Ghiso, J., and Frangione, B. (1991) *Biochem. Biophys. Res. Commun.* **173**, 1247–1254
- Castaño, E. M., Prelli, F., Wisniewski, T., Golabek, A., Kumar, R. A., Soto, C., and Frangione, B. (1995) *Biochem. J.* **306**, 599–604
- Van Nostrand, W. E., Melchor, J. P., Cho, H. S., Greenberg, S. M., and Rebeck, G. W. (2001) *J. Biol. Chem.* **276**, 32860–32866
- De Jonghe, C., Zehr, C., Yager, D., Prada, C. M., Younkin, S., Hendriks, L., Van Broeckhoven, C., and Eckman, C. B. (1998) *Neurobiol. Dis.* **5**, 281–286
- Walsh, D. M., Hartley, D. M., Condrón, M. M., Selkoe, D. J., and Teplow, D. B. (2001) *Biochem. J.* **355**, 869–877
- Melchor, J. P., McVoy, L., and Van Nostrand, W. E. (2000) *J. Neurochem.* **74**, 2209–2212
- Gau, J. T., Steinhilb, M. L., Kao, T. C., D'Amato, C. J., Gaut, J. R., Frey, K. A., and Turner, R. S. (2002) *Am. J. Pathol.* **160**, 731–738
- Kuo, Y. M., Beach, T. G., Sue, L. I., Scott, S., Layne, K. J., Kokjohn, T. A., Kalback, W. M., Luehrs, D. C., Vishnivetskaya, T. A., Abramowski, D., Sturchler-Pierrat, C., Staufenbiel, M., Weller, R. O., and Roher, A. E. (2001) *Mol. Med.* **7**, 609–618
- Iwata, N., Tsubuki, S., Takaki, Y., Shirohata, K., Lu, B., Gerard, N. P., Gerard, C., Hama, E., Lee, H. J., and Saido, T. C. (2001) *Science* **292**, 1550–1552
- Eckman, E. A., Reed, D. K., and Eckman, C. B. (2001) *J. Biol. Chem.* **276**, 24540–24548
- Selkoe, D. J. (2001) *Neuron* **32**, 177–180
- Carson, J. A., and Turner, A. J. (2002) *J. Neurochem.* **81**, 1–8
- Baumeister, H., Müller, D., Rehbein, M., and Richter, D. (1993) *FEBS Lett.* **317**, 250–254
- Kuo, W., Montag, A. G., and Rosner, M. R. (1993) *Endocrinology* **132**, 604–611
- Becker, A. B., and Roth, R. A. (1992) *Proc. Natl. Acad. Sci. U. S. A.* **89**, 3835–3839
- Bennett R. G., Hamel F. G., and Duckworth W. C. (2000) *Endocrinology* **141**, 2508–2517
- Authier, F., Posner, B. I., and Bergeron, J. J. M. (1996). *Clin. Invest. Med.* **19**, 149–158
- Kurochkin, I. V., and Goto, S. (1994) *FEBS Lett.* **345**, 33–37
- Bennett R. G., Duckworth W. C., and Hamel F. G. (2000) *J. Biol. Chem.* **275**, 36621–36625
- Kurochkin, I. V. (2001) *Trends Biochem. Sci.* **26**, 421–425
- McDermott, J. R., and Gibson, A. M. (1997) *Neurochem. Res.* **22**, 49–56
- Perez, A., Morelli, L., Cresto, J. C., and Castaño, E. M. (2000) *Neurochem. Res.* **25**, 247–255
- Qiu, W. Q., Walsh, D. M., Ye, Z., Vekrellis, K., Zhang, J., Podlisny, M. B., Rosner, M. R., Safavi, A., Hersch, L. B., and Selkoe, D. J. (1998) *J. Biol. Chem.* **273**, 32730–32738
- Gasparini, L., Gouras, G. K., Wang, R., Gross, R. S., Beal, M. F., Greengard, P., and Xu, H. (2001) *J. Neurosci.* **21**, 2561–2570
- Mukherjee, A., Song, E., Kihiko-Ehmann, M., Goodman, J. P., St. Pyrek, J., Estus, E., and Hersch, L. B. (2000) *J. Neurosci.* **20**, 8745–8749
- Walsh, D. M., Klyubin, I., Fadeeva, J. V., Cullen, W. K., Anwyl, R., Wolfe, M. S., Rowan, M. J., and Selkoe, D. A. (1992) *Biochemistry* **31**, 10716–10723
- Chesneau, V., and Rosner, M. R. (2000) *Protein Expression Purif.* **19**, 91–98
- Fraser, P. E., Nguyen, J. T., Inouye, H., Surewicz, W. K., Selkoe, D. J., Podlisny, M. B., and Kirschner, D. A. (1992) *Biochemistry* **31**, 10716–10723
- Castaño, E. M., Prelli, F., Soto, C., Beavis, R., Matsubara, E., Shoji, M., and Frangione, B. (1996) *J. Biol. Chem.* **271**, 32185–32191
- Duckworth, W. C., Hamel, F. G., Bennett, R., Ryan, M. P., and Roth, R. A. (1990) *J. Biol. Chem.* **265**, 2984–2987
- Pirttila, T., Kim, K. S., Mehta, P. D., Frey, H., and Wisniewski, H. M. (1994) *J. Neurol. Sci.* **127**, 90–95
- Chesneau, V., Vekrellis, K., Rosner, M. R., and Selkoe, D. J. (2000) *Biochem. J.* **351**, 509–516
- Song, E. S., Mukherjee, A., Juliano, M. A., Pyrek, J. S., Goodman, J. P., Jr, Juliano, L., and Hersch, L. B. (2001) *J. Biol. Chem.* **276**, 1152–1155
- Pallitto, M. M., and Murphy, R. M. (2001) *Biophys. J.* **81**, 1805–1822
- Prelli, F., Levy, E., van Duinen, S. G., Bots, G. T., Luyendijk, W., and Frangione, B. (1990). *Biochem. Biophys. Res. Commun.* **170**, 301–307
- Zhang, S., Iwata, K., Lachenmann, M. J., Peng, J. W., Li, S., Stimson, E. R., Lu, Y., Felix, A. M., Maggio, J. E., and Lee, J. P. (2000) *J. Struct. Biol.* **30**, 130–141
- Massi, F., and Straub, J. E. (2001) *Biophys. J.* **81**, 697–709
- Hilbich, C., Kisters-Woike, B., Reed, J., Masters, C. L., and Beyreuther, K. (1992) *J. Mol. Biol.* **228**, 460–473
- Soto, C., Castaño, E. M., Frangione, B., and Inestrosa, N. C. (1995) *J. Biol. Chem.* **270**, 3063–3067
- Balbach, J. J., Ishii, Y., Antzutkin, O. N., Leapman, R. D., Rizzo, N. W., Dyda, F., Reed, J., and Tycko, R. (2000) *Biochemistry* **39**, 13748–13759
- Kurochkin, I. V. (1998) *FEBS Lett.* **427**, 153–156
- Callahan, M. J., Lipinski, W. J., Bian, F., Durham, R. A., Pack, A., and Walker, L. C. (2001) *Am. J. Pathol.* **158**, 1173–1177
- Bading, J. R., Yamada, S., Mackic, J. B., Kirkman, L., Miller, C., Calero, M., Ghiso, J., Frangione, B., and Zlokovic, B. V. (2002) *J. Drug Target.* **10**, 359–368
- Monro, O., Mackic, J., Yamada, S., Segal, M., Ghiso, J., Maurer, C., Calero, M., Frangione, B., and Zlokovic, B. (2002) *Neurobiol. Aging* **23**, 405–412
- Cook, D. G., Leverenz, J. B., McMillan, P. J., Kulstad, J. J., Erickson, S., Roth, R. A., Schellenberg, G. D., Jin, L. W., Kovacina, K. S., and Craft, S. (2003) *Am. J. Pathol.* **162**, 313–319
- Saido, T. C., Tsubuki, S., Takaki, Y., Huang, S. M., Saito, T., and Iwata, N. (2002) *Society for Neuroscience*, Washington, D. C., Abstract program number 624.12